Density-functional calculation of sub-band structure in accumulation and inversion layers

T. Ando*
Physik-Department der Technischen Universität München, 8046 Garching-bei-München, West Germany
(Received 9 September 1975)

The Hohenberg-Kohn-Sham theory of an inhomogeneous electron gas is applied to the calculation of the sub-band structure of accumulation and inversion layers on the Si (100) surface. The exchange-correlation effect is shown to be very important and lower the sub-band energies considerably. Especially in accumulation layers the first excited sub-band really becomes a bound state in contrast to the result of the Hartree approximation. The agreement between the theory and experimental results of inter-sub-band optical transitions is satisfactory. The effective mass and the g factor are also calculated.

I. INTRODUCTION

When a strong electric field is applied perpendicularly to a surface of a semiconductor, the electronic states form two-dimensional energy bands called electric sub-bands. Each sub-band describes a quantized motion normal to the surface, with a continuum for motion in the plane parallel to the surface. The structure of the sub-bands has usually been calculated within the framework of the so-called self-consistent Hartree approximation.[1-3] Stern[4] made an extensive calculation for n-channel inversion layers on Si. He also calculated the sub-band structure of an n-channel accumulation layer on Si.[5] Effects of strong magnetic fields applied parallel to the surface and the image potential arising from the existence of the oxide layer have been investigated previously.[6] Bangert *et al.*[7] and Ohkawa and Uemura[8] have performed a calculation in p-channel inversion layers on Si.

Since the electron concentration of the system can be controlled over a wide range, this system provides a useful tool for studying effects of mutual Coulomb interactions. There have been a number of experimental and theoretical studies on the g factor (g^*) and the effective mass (m^*).[9-19] Recently a direct observation of optical transitions between different electric sub-bands has become possible,[20-23] and insufficiencies of the self-consistent Hartree approximation have been pointed out through comparison between theoretical and experimental results.[6,22,23] A many-body effect such as the exchange and correlation can strongly affect the structure of the sub-bands. Stern[24,25] calculated the exchange energy in the lowest-order perturbation and has shown that the energy of the ground sub-band is considerably lowered. Vinter[18] calculated the energy of the ground and the first excited sub-band including the correlation effect within a perturbation method based on the result of the self-consistent Hartree approximation. Effects of the finite thickness of accumulation and inversion layers have been pointed out to be important, which means that mixing between different sub-bands owing to the exchange-correlation effect can play an important role.

There is an entirely different approach to these problems, i.e., the density-functional formulation based on the theory of an inhomogeneous electron gas developed by Hohenberg, Kohn, and Sham.[26-28] This theory has been used and tested in a number of problems such as the investigation of properties of metal surfaces and the band calculation of metals.[29] In this paper we apply it to the present problems of surface layers. We calculate the charge density, the self-consistent potential, the quasiparticle properties such as m^* and g^*, and the sub-band structure in n-channel accumulation and inversion layers on a Si (100) surface.

In Sec. II we briefly discuss the approximation scheme and the procedure of the calculation. We neglect the anisotropy of the conduction band of Si and obtain a self-energy shift of a uniform three-dimensional electron gas within a Hubbard-like approximation. The image effect on the mutual Coulomb interaction is included in a certain approximation. Using the obtained self-energy shift, we calculate the sub-band structure. In Sec. III the results and some discussions on them are given, and they are compared with the results of the Hartree calculation and with experiments.

II. PROCEDURE OF CALCULATION

Hohenberg, Kohn, and Sham[26,27] have shown that the density distribution of an interacting electron gas under an external field can be obtained by a one-body Schrödinger-type equation containing an exchange-correlation potential v_{xc} in addition to the usual Hartree potential and the external potential. Such an exchange-correlation potential v_{xc} is given by taking a functional derivative of the exchange-correlation part of the ground-state energy E_{xc} with respect to the number density $n(\vec{r})$ of electrons. The functional form of $E_{xc}[n(\vec{r})]$ is not known and is replaced by a product $n(\vec{r})\epsilon_{xc}(n(\vec{r}))$ in the usual local approximation, where $\epsilon_{xc}(n)$ is the exchange-correlation energy per electron of a uniform elec-

tron gas with the density n. In this approximation $v_{xc}(\vec{r})$ becomes the exchange-correlation part of the chemical potential μ_{xc} of the uniform electron gas.

Such theory can easily be applied to the present problem. One has to add $v_{xc}(z)$ to the usual self-consistent Hartree equation, where z is the distance into the bulk measured from the surface. It is sufficient to confine ourselves to the sub-bands associated with the two valleys which present the highest mass for motion perpendicular to the surface. These have the lowest kinetic energy and the lowest energy levels, and only the lowest sub-band is usually occupied by electrons at zero temperature. The Schrödinger-type-equation is written

$$\left(\frac{\hbar^2}{2m_t}\vec{k}^2 - \frac{\hbar^2}{2m_l}\frac{\partial^2}{\partial z^2} + V_{\text{eff}}(z)\right)\xi_n(z)e^{i\vec{k}\cdot\vec{r}} = \epsilon_n(k)\xi_n(z)e^{i\vec{k}\cdot\vec{r}}, \quad (2.1)$$

where $\vec{k} = (k_x, k_y)$ and $\vec{r} = (x, y)$ represent two-dimensional vectors in the plane (xy plane) parallel to the surface, and m_t and m_l are the effective mass in the direction parallel and perpendicular to the surface, respectively. The effective potential $V_{\text{eff}}(z)$ consists of the usual electrostatic potential $v(z)$ including the Hartree potential of electrons themselves and the exchange-correlation potential $v_{xc}(z)$. One can decompose $v(z)$ into

$$v(z) = v_{\text{depl}}(z) + v_{\text{image}}(z) + v_S(z), \quad (2.2)$$

with

$$v_{\text{depl}}(z) = \begin{cases} (4\pi e^2/\kappa_{sc})N_{\text{depl}}z(1 - z/2z_d), \\ (4\pi e^2/\kappa_{sc})N_{\text{depl}}\tfrac{1}{2}z_d, \end{cases} \quad (2.3)$$

$$v_{\text{image}}(z) = \frac{\kappa_{sc} - \kappa_{ox}}{4\kappa_{sc}(\kappa_{sc} + \kappa_{ox})}\frac{e^2}{z}, \quad (2.4)$$

and

$$v_S(z) = \frac{4\pi e^2}{\kappa_{sc}}\left(N_S z - \int_0^z (z - z')n(z')\,dz'\right), \quad (2.5)$$

where $N_{\text{depl}} = N_A z_d$, $z_d = (\kappa_{sc}|E_B|/2\pi e^2 N_A)^{1/2}$, κ_{sc} and κ_{ox} are the static dielectric constant of silicon and its oxide, respectively, N_S is the concentration of surface electrons in a unit area, E_B is the Fermi energy in the bulk measured from the conduction band edge, and N_A is the concentration of the fixed space charges in the region where the band is bent down. In case of an accumulation layer N_A is the acceptor concentration, and in case of an inversion layer N_A is the acceptor concentration minus the donor concentration. The density distribution is given by

$$n(z) = n_v n_s \sum_{\text{occupied}(n,\vec{k})} |\xi_n(z)|^2, \quad (2.6)$$

where n_v and n_s are the valley and the spin degeneracy, respectively.

In order to get $v_{xc}(z)$ one has to calculate μ_{xc} of an electron gas characterized by anisotropic masses m_t and m_l. As has been discussed by several authors, however, such an anisotropy effect is expected to be small in Si.[30,31] Therefore, one replaces μ_{xc} by the chemical potential of an electron gas which consists of electrons with an isotropic mass m_{op}, defined by

$$\frac{1}{m_{op}} = \frac{1}{3}\left(\frac{2}{m_t} + \frac{1}{m_l}\right). \quad (2.7)$$

One has to include the interaction with images of other electrons because of the existence of the oxide layer with a different dielectric constant. The electron-electron interaction is given by

$$V(\vec{r}_1 z_1; \vec{r}_2, z_2) = \frac{e^2}{\kappa_{sc}[(\vec{r}_1 - \vec{r}_2)^2 + (z_1 - z_2)^2]^{1/2}} + \frac{\kappa_{sc} - \kappa_{ox}}{\kappa_{sc}(\kappa_{sc} + \kappa_{ox})}\frac{e^2}{[(\vec{r}_1 - \vec{r}_2)^2 + (z_1 - z_2)^2 + 4z_1 z_2]^{1/2}}. \quad (2.8)$$

Since we are employing the local approximation, we expect that the image effect is taken into account to a great extent in the following manner. That is, $v_{xc}(z)$ is replaced by μ_{xc} of an electron gas where the mutual interaction between electrons at $(\vec{r}_1, z_1)$ and $(\vec{r}_2, z_2)$ is given by

$$V(\vec{r}_1, z_1; \vec{r}_2, z_2; z) = \frac{e^2}{\kappa_{sc}[(\vec{r}_1 - \vec{r}_2)^2 + (z_1 - z_2)^2]^{1/2}} \times \frac{\kappa_{sc} - \kappa_{ox}}{\kappa_{sc}(\kappa_{sc} + \kappa_{ox})}\frac{e^2}{[(\vec{r}_1 - \vec{r}_2)^2 + (z_1 - z_2)^2 + 4z^2]^{1/2}}. \quad (2.9)$$

The exchange-correlation potential v_{xc} becomes dependent on z explicitly. Since μ_{xc} is related to the quasiparticle energy at the Fermi surface through

$$\mu_{xc} = \epsilon(k_F) - \frac{\hbar^2 k_F^2}{2m_{op}} \equiv \Delta\epsilon(k_F), \quad (2.10)$$

one has to calculate the self-energy of electrons. In this paper we take into account those diagrams shown in Fig. 1, in which the vertex correction is included in a Hubbard-like approximation.[32] Details of the calculation are given in the Appendix. Examples of the results of a numerical calculation are shown in Fig. 2, where $\mu_{xc}(r_s, a)$ is shown for several a as a function of r_s, defined by $\alpha r_s = 1/a_B^* k_F$, $\alpha = (2n_v n_s/9\pi)^{1/3}$, and $a_B^* = \kappa\hbar^2/m_{op}e^2$,

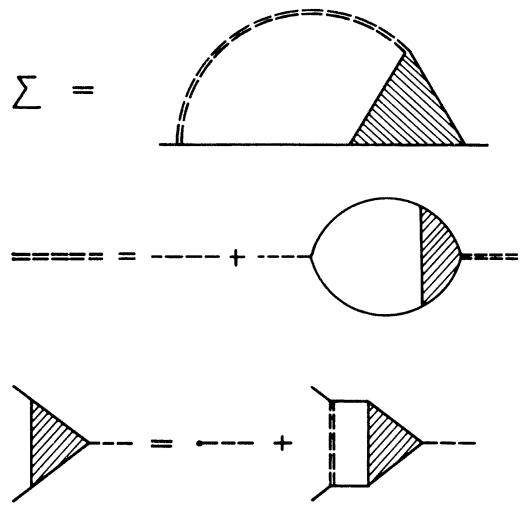

FIG. 1. Approximation scheme in the calculation of the self-energy. Vertex correction is included in a manner discussed by Hubbard, and the Coulomb interaction in the vertex correction is screened by the Thomas-Fermi dielectric function.

where $\bar{\kappa}=\frac{1}{2}(\kappa_{sc}+\kappa_{ox})$ and $a=2k_F z$. Strictly speaking, the energy eigenvalue $\epsilon_n(k)$ obtained from Eq. (2.1) does not represent the quasiparticle energy. Sham and Kohn[28] proposed a local energy-dependent exchange-correlation potential which gives quasiparticle energies. According to their theory one should use the self-energy shift $\Delta\epsilon(k)$ which satisfies

$$\Delta\epsilon(k)+\frac{\hbar^2k^2}{2m_{op}}=E-\mu+\frac{\hbar^2k_F^2}{2m_{op}}+\mu_{xc}\,, \tag{2.11}$$

instead of μ_{xc}, where E is the energy of a quasiparticle and μ is the chemical potential in the surface layer. The properties of quasiparticles near the chemical potential can be derived in the lowest-order perturbation, and m^* is given by

$$m^*=\frac{m_t}{m_{op}}\int_0^\infty m^*(n(z);z)\,n(z)\,dz\left(\int_0^\infty n(z)\,dz\right)^{-1}. \tag{2.12}$$

If one makes a similar argument, one gets the following expression for g^* under weak magnetic fields:

$$g^*=\frac{1}{m^*}\int_0^\infty m^*(n(z);z)\,g^*(n(z);z)\,n(z)\,dz\left(\int_0^\infty n(z)\,dz\right)^{-1}, \tag{2.13}$$

where $m^*(n(z);z)$ and $g^*(n(z);z)$ are the effective mass enhancement factor and the g factor, respectively, of the uniform electron gas. These quantities $m^*(r_s;a)$ and $g^*(r_s;a)$ are also calculated in the Appendix and the results are shown in Figs. 3 and 4.

The self-energy shift $\Delta\epsilon(k)$ in the case of $a=0$ is shown in Fig. 5 as a function of $(k/k_F)^2$ together with the exchange energy calculated in the Hartree-Fock approximation. The k dependence of the self-energy and consequently the energy dependence of the potential is important in the exchange-only approximation, and higher sub-bands are not so much affected by the exchange interaction compared with the ground sub-band.[25] The energy dependence of the potential becomes much smaller when the correlation effect is taken into account. One might be able to use this result in calculating the sub-band structure. However, such a calculation requires long and tedius computer work, and further it is expected to give a result not so much differ-

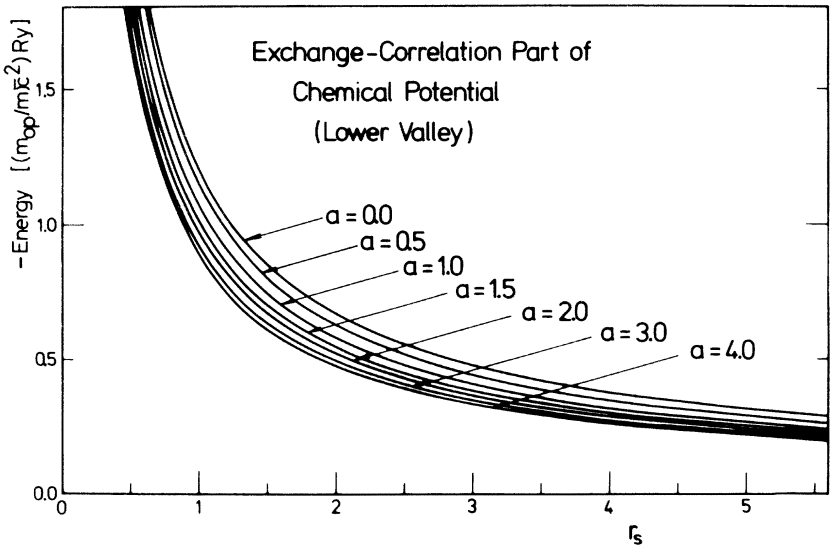

FIG. 2. Exchange-correlation part of the chemical potential μ_{xc} of a homogeneous electron gas where the mutual interaction is given by Eq. (2.9).

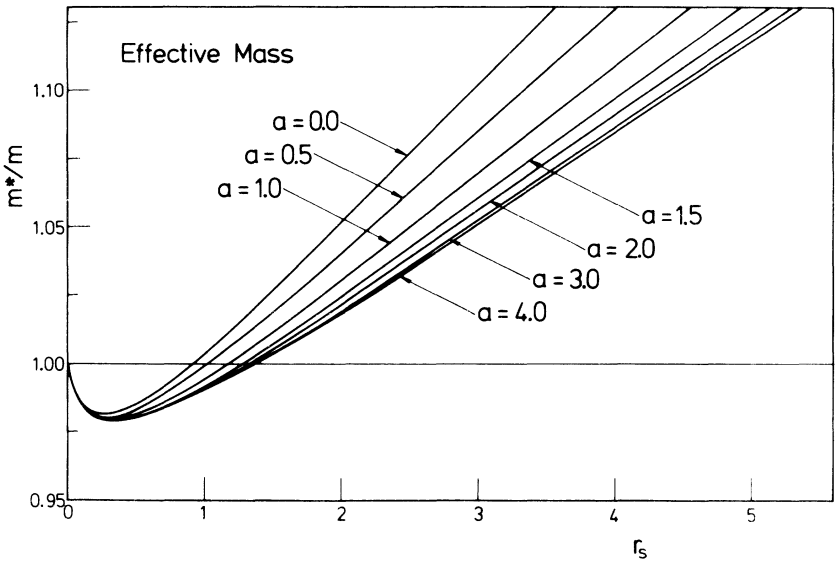

FIG. 3. Enhancement of the effective mass of a homogeneous electron gas.

ent from that obtained by the use of the energy independent $v_{eff}(z)$.[33] In this paper, therefore, one uses $v_{eff}(z)$ in calculating the energy of the subbands associated with the lower two valleys. In order to calculate the energy spectra of the subbands associated with the different four valleys one has to use a different exchange-correlation potential. According to the theory of Sham and Kohn[28] one should use the self-energy shift $\Delta\epsilon'(k)$ of an electron of these four valleys, which satisfies the same equation as Eq. (2.11). This energy shift is also calculated in a similar approximation in the Appendix. Examples of the results in the case of $a = 0$ are shown in Fig. 6. In the exchange-only approximation, there is no energy shift because there is no electron in these valleys. If one includes the correlation effect, however, one gets an energy shift comparable to that of electrons in the lower two valleys. We again neglect the energy dependence and use here $\Delta\epsilon'(k=0)$. Examples of obtained $\Delta\epsilon'(0)$ are shown in Fig. 7. Since the k dependence of $\Delta\epsilon'(k)$ is larger than that of $\Delta\epsilon(k)$, the neglect of the dependence is less justified in case of $\Delta\epsilon'(k)$.

By using the numerical results one can construct an interpolation formula of $v_{xc}(r_s; a)$, $m^*(r_s; a)$, and $m^*g^*(r_s; a)$ which covers an important region of r_s ($0.5 \lesssim r_s \lesssim 7$) and can be extrapolated into the region of r_s larger than seven. After getting such a formula one can easily solve the

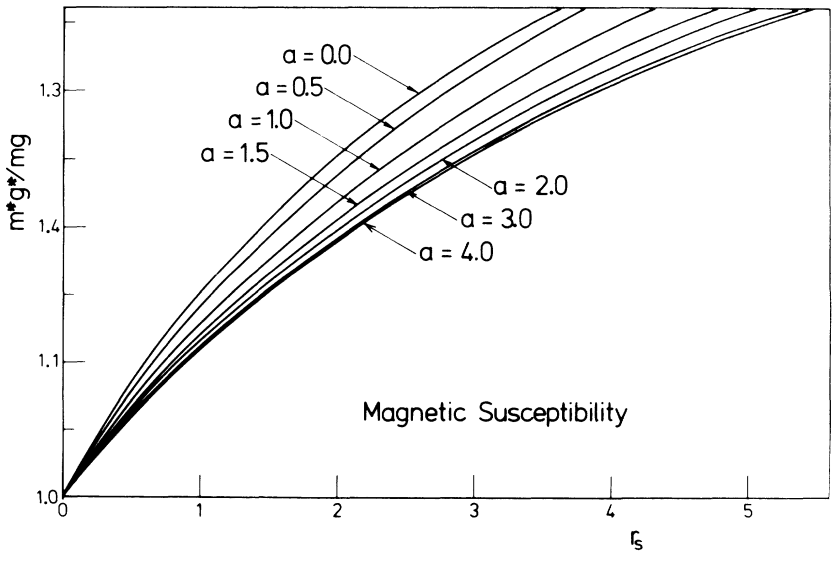

FIG. 4. Enhancement of the spin susceptibility of a homogeneous electron gas.

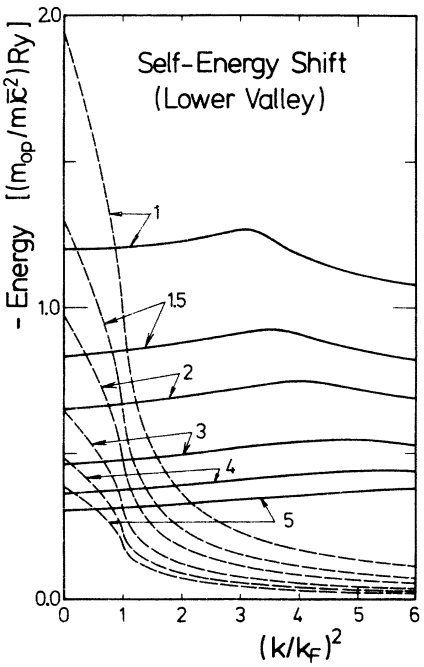

FIG. 5. Quasiparticle energy shift $\Delta\epsilon(k)$ of a homogeneous electron gas ($a=0$). Broken lines represent the results of the Hartree-Fock approximation and the solid lines the present results. Numbers in the figure represent values of r_s.

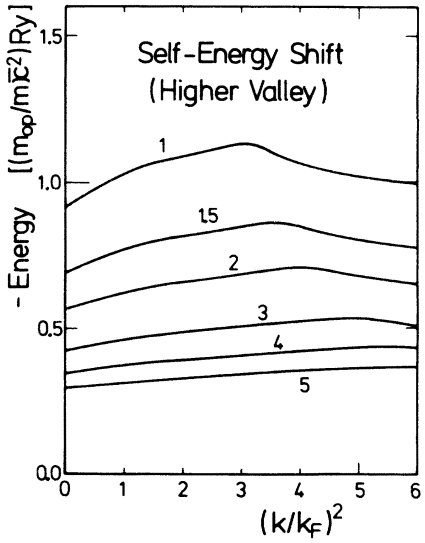

FIG. 6. Quasiparticle energy shift $\Delta\epsilon'(k)$ of an electron in the higher four valleys ($a=0$). Hartree-Fock approximation gives $\Delta\epsilon'(k)=0$.

self-consistent equation numerically in a similar manner described earlier.[6] The results of such a calculation are presented in Sec. III.

III. RESULTS AND DISCUSSION

Here one uses the values, $m_t=0.195m$, $m_l=0.916m$, $n_v=n_s=2$, $\kappa_{sc}=11.8$, and $\kappa_{ox}=3.8$, where m is the mass of a free electron. An example of the self-consistent potential and the electron density in case of accumulation ($N_A=1.0\times10^{14}$ cm^{-3}, $E_B=-45$ meV, $N_{depl}=7.7\times10^{9}$ cm^{-2}, and $N_s=1.0\times10^{12}$ cm^{-2}) is shown in Fig. 8 together with the result of the Hartree approximation. The energy of each sub-band is lowered considerably. The exchange-correlation effect is equally important for higher excited sub-bands in contrast to the result of the Hartree-Fock approximation.[25] The spatial extent of the electron density becomes smaller and the structure of the sub-bands is

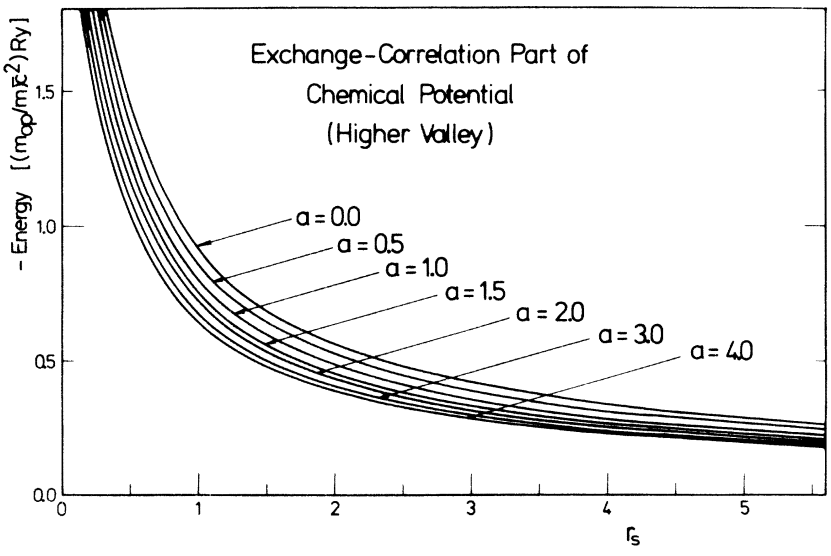

FIG. 7. Quasiparticle energy shift $\Delta\epsilon'(k=0)$ of an electron in the higher four valleys as a function of r_s.

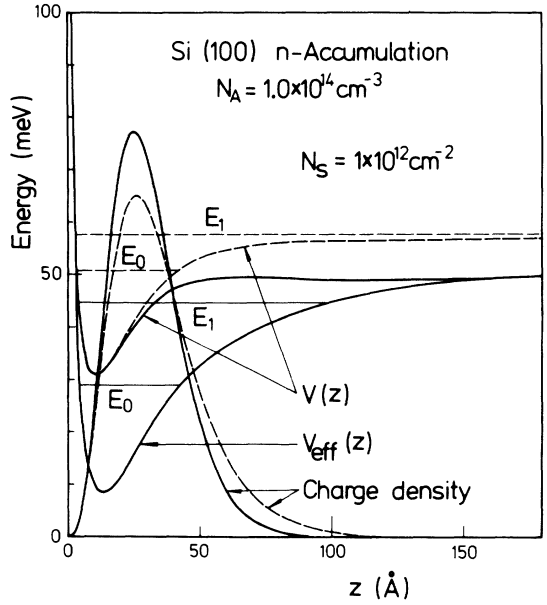

FIG. 8. Charge-density distribution of electrons, the self-consistent potential, and the edges of the sub-bands in an accumulation layer ($N_{depl} = 7.7\times10^{9}$ cm^{-2}). Broken lines represent the result of the Hartree approximation and the solid lines the present result.

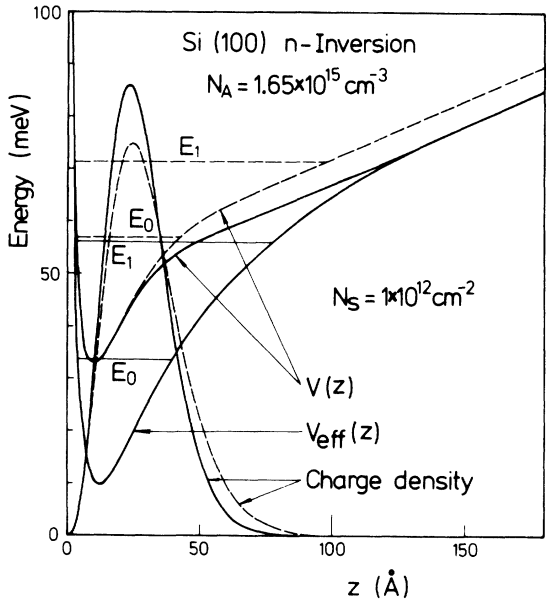

FIG. 10. Charge-density distribution of electrons, the self-consistent potential, and the bottom of the sub-bands in an inversion layer ($N_{depl} = 1.55\times10^{11}$ cm^{-2}). Broken lines represent the result of the Hartree approximation and the solid lines the present result.

strongly modified. This shows that mixing between different sub-bands is large and that a perturbational calculation including only a single sub-band is not satisfactory in the accumulation case. In the Hartree approximation only the ground sub-band is localized in the surface region, and all other sub-bands become more extended and are quasicontinuum states. Consequently, a line shape of inter-sub-band optical transitions either has structure corresponding to transitions from the ground to excited sub-bands or is very broadened, depending on the strength of scattering from impurities and surface roughness. When the exchange-correlation effect is taken into account, the first excited sub-band becomes also localized in the surface region. One can expect that the line shape becomes sharp. This is consistent with the experimental results of Kamgar *et al.*[20,21] who observed a very narrow line shape similar to that observed in an inversion layer.[23] The energy of the edge of each sub-band measured from that of the ground sub-band is shown in Fig. 9. This again shows the importance of the exchange-correlation effect clearly.

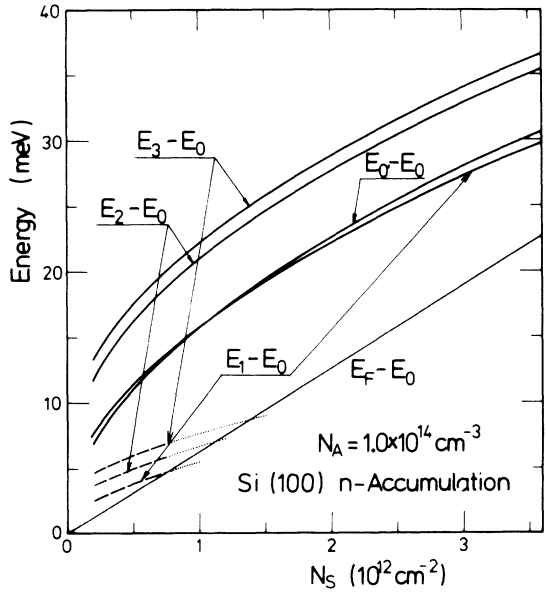

FIG. 9. Sub-band energies and the Fermi energy measured from the bottom of the ground sub-band in an accumulation layer (see Fig. 8). Broken lines represent the result of the Hartree approximation and the solid lines the present result.

An example for an inversion layer ($N_A = 1.65\times10^{15}$ cm^{-3}, $E_B = -1.12$ eV, $N_{depl} = 1.55\times10^{11}$ cm^{-2}, and $N_S = 1.0\times10^{12}$ cm^{-2}) is shown in Figs. 10 and 11. Since there is a strong electric field of fixed space charges, the structure of the sub-bands and the electron density are not so much altered as in the accumulation case.[25] However, energies of the sub-bands are strongly lowered by the exchange-correlation effect. The decrease of the energy of the ground sub-band and of the first excited sub-

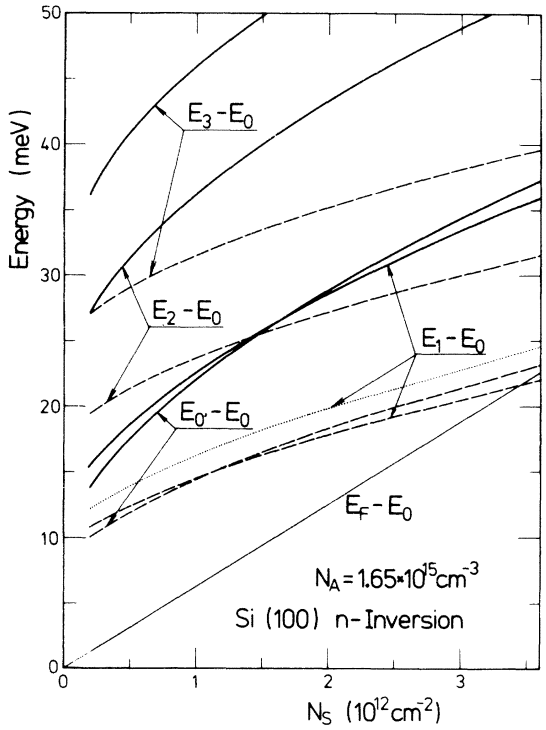

FIG. 11. Sub-band energies and the Fermi energy measured from the bottom of the ground sub-band in an inversion layer (see Fig. 10). Broken lines represent the result of the Hartree approximation and the solid lines the present result. Dotted curve represents the result of the Hartree approximation in which the image effect is neglected.

band is larger than that of Vinter[18] who calculated the energy shift perturbationally starting from Stern's Hartree result. The energy of the lowest sub-band E_0' associated with the higher four valleys is almost the same as that of the first excited sub-band of the lower two valleys. This is a similar behavior as the result of the Hartree approximation.[4]

The effective mass m^* is shown in Fig. 12. For accumulation the mass is slightly larger than for inversion. If the mass is calculated perturbationally by including only the ground sub-band, it becomes larger in the inversion case, since the spatial extent of the electron density is smaller and the effective Coulomb interaction is larger in the inversion case. It is not clear whether this difference relates to the mixing between different sub-bands or whether it relates to an insufficiency of the Hohenberg-Kohn-Sham theory. The present result is larger than that of Vinter,[18] but is still smaller than the experimental results of Smith and Stiles.[10] Recently Lee *et al.*[19] also calculated the mass neglecting the mixing. Their result is larger than the present one.

The effective g factor under weak magnetic fields is also shown in Fig. 12. The present result is slightly smaller than that of Ando and Uemura,[16] but its N_S dependence is similar. At very low electron concentrations g^* decreases with the decrease of the concentration. This behavior is similar to the result obtained by Ting *et al.*[17] and is thought to arise from an insufficient vertex correction in the approximation of the self-energy. The predicted N_S dependence of g^* is the same as experimentally observed by Fang and Stiles,[9] and by Kobayashi and Komatsubara.[12] However, the absolute value of g^* cannot directly be compared with the experiments, since the experiments have been performed under strong magnetic fields. Under strong magnetic fields one has to take into account the singular nature of the density of states.[16]

Since the thickness z_d of the fixed space-charge layer is much larger than the thickness of accumulation and inversion layers, the sub-band structures is determined only by the value of N_{depl} irrespectively of each value of N_A and E_B. The energy splitting between the ground and the first ex-

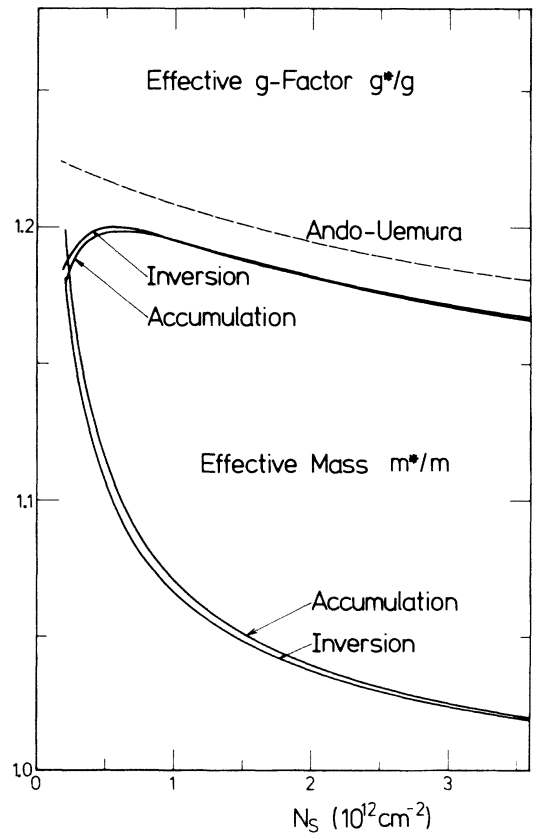

FIG. 12. Enhancement of the effective mass and the g factor. The g factor obtained by Ando and Uemura (Ref. 16) is also shown for the sake of comparison.

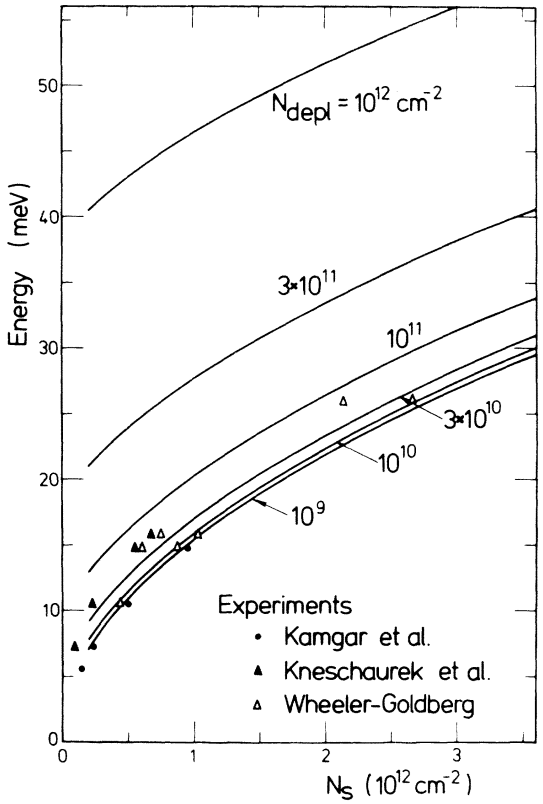

FIG. 13. Energy splitting between the ground and the first-excited sub-band for several N_{depl}. Experimental results in an accumulation layer (Refs. 20, 21), in an inversion layer (△, $N_{depl}=1.8\times10^{11}$ cm^{-2}) (Ref. 23) and the results of photoconductivity measurements in an inversion layer (△, $N_{depl}=1.0\times10^{11}$ cm^{-2}) are also shown. Photoconductive response gives two peaks.

cited sub-band is plotted as a function of N_S for several N_{depl} in Fig. 13. In case of small N_{depl} ($\lesssim 10^{10}$ cm^{-2}) corresponding to the accumulation case, the energy splitting is determined by the potential of electrons themselves and is almost independent of N_{depl}. If one neglects the so-called vertex correction, the energy of the inter-sub-band optical transition becomes the same as the energy splitting shown in Fig. 13. The experimental results for accumulation[20,21] are shown in Fig. 13. The N_S dependence of the theoretical and the experimental results is the same, and their absolute values agree with each other. The experimental results for inversion ($N_{depl}=1.8\times10^{11}$ cm^{-2}) (Ref. 23) are also shown. The calculated energies are larger than the experimental values, but the N_S dependence is almost the same. Wheeler and Goldberg[34] measured photoconductivity and observed two peaks in the photoconductive response. Their results are also shown in Fig. 13. The two peaks show the same N_S dependence as the theory, but such a two-peaked structure cannot be explained by the present theory. The neglect of the vertex correction might not be fully justified in our system, if one considers the importance of the many-body exchange-correlation effect. One can conclude, however, that the agreement between theory and experiment is satisfactory at the present stage.

Recently there have been many attempts to include nonlocal terms such as a gradient of the effective potential in the Hohenberg-Kohn-Sham theory, and there has been criticism on the local theory.[35] The applicability of such local theory should also be checked through comparison with various experiments. Our system is suited for such kind of investigations.

ACKNOWLEDGMENTS

The author is grateful to Professor J. F. Koch and Dr. A. Kamgar for many valuable discussions. I wish to thank Professor J. F. Koch and all the members of Physik-Department der Technischen Universität München for their hospitality.

APPENDIX: CALCULATION OF A SELF-ENERGY SHIFT

When one includes the diagram shown in Fig. 1 and employs a Hubbard-like approximation, one gets the following expression for the shift in the quasiparticle energy of an electron with a momentum k, a spin σ, and a valley index v:

$$\Sigma_{\sigma v}\left(\vec{k}, \frac{\hbar^2k^2}{2m_{op}}\right) = \sum_q \int \frac{d\omega}{2\pi i} V(q) \frac{\Gamma_{\sigma v}(q,\omega)}{\epsilon(q,\omega)} G_0^{\sigma v}\left(\vec{k}+\vec{q}, \frac{\hbar^2k^2}{2m_{op}}+\omega\right), \tag{A1}$$

with

$$G_0^{\sigma v}(\vec{k},\epsilon) = \frac{n_{k\sigma v}}{\epsilon - \hbar^2k^2/2m_{op} - i0} + \frac{1-n_{k\sigma v}}{\epsilon - \hbar^2k^2/2m_{op} + i0}, \tag{A2}$$

$$\epsilon(q,\omega) = 1 + V(q)\sum_{\sigma v} \Pi_{\sigma v}(q,\omega)\Gamma_{\sigma v}(q,\omega), \tag{A3}$$

$$\Gamma_{\sigma v}(q,\omega)^{-1} = 1 - \frac{V[(q^2+k_F^2)^{1/2}]}{\epsilon_{TF}[(q^2+k_F^2)^{1/2}]}\Pi_{\sigma v}(q,\omega), \tag{A4}$$

and

$$\Pi_{\sigma v}(q,\omega) = \sum_{\vec{k}} \int \frac{d\epsilon}{2\pi i} G_0^{\sigma v}(\vec{k},\epsilon) G_0^{\sigma v}(\vec{k}+\vec{q},\epsilon+\omega), \tag{A5}$$

where $n_{k\sigma v}=1$ for $k<k_F$, $n_{k\sigma v}=0$ for $k>k_F$, and the vectors used here are three dimensional. The Coulomb matrix element $V(q)$ is the Fourier transform of Eq. (2.9) and is given by

$$V(q) = \frac{4\pi e^2}{\bar{\kappa}q^2}\left[\frac{1}{2}\left(1+\frac{\kappa_{ox}}{\kappa_{sc}}\right)+\frac{1}{2}\left(1-\frac{\kappa_{ox}}{\kappa_{sc}}\right)2qz\,K_1(2qz)\right] \equiv \frac{4\pi e^2}{\bar{\kappa}q^2}F(2qz), \tag{A6}$$

where $K_1(x)$ is a modified Bessel function. The Thomas-Fermi dielectric function $\epsilon_{TF}(q)$ is given by

$$\epsilon_{TF}(q) = 1 + V(q) \lim_{q \to 0} \sum_{\sigma\nu} \Pi_{\sigma\nu}(q, 0) \ . \tag{A7}$$

As has been discussed by Rice,[36] one should replace the energy variable in the self-energy by a free value $\hbar^2 k^2/2m_{op}$ in case that only the lowest diagrams are included. After a little manipulation one gets

$$\mu_{xc}(r_s; z) = \Sigma\left(k_F, \frac{\hbar^2 k_F^2}{2m_{op}}\right) = \frac{m_{op}}{m\kappa^2}\left[-\frac{2}{\pi\alpha r_s}\int_0^2 F(qa)(1-\tfrac{1}{2}q)\,dq - \frac{2}{\pi\alpha r_s}\int_0^\infty dq \int_0^\infty \frac{d\omega}{2\pi} \times F(qa)\left(1 - \frac{1}{\epsilon_s(q, i\omega q)}\right) \ln\frac{(2+q)^2+\omega^2}{(2-q)^2+\omega^2}\right] \mathrm{Ry} \ , \tag{A8}$$

where the length and the energy are measured in units of k_F^{-1} and $\hbar^2 k_F^2/2m_{op}$, respectively, and

$$\epsilon_s(q, i\omega q) = 1 + \frac{2}{\pi}\alpha r_s\left(\frac{n_v n_s}{q^2} F(q\beta) - \frac{F[(q^2+1a)^{1/2}]}{q^2 + 1 + (2/\pi) n_v n_s \alpha r_s F[(q^2+1)^{1/2}a]}\right) \Pi_0(q, i\omega q) \ , \tag{A9}$$

with

$$\Pi_0(q, i\omega q) = \frac{1}{2} + \frac{\omega^2 + 4 - q^2}{16q} \ln\frac{(q+2)^2+\omega^2}{(q-2)^2+\omega^2} - \frac{\omega}{4}\left(\tan^{-1}\frac{2+q}{\omega} + \tan^{-1}\frac{2-q}{\omega}\right) \ . \tag{A10}$$

As for the effective mass m^*, one gets

$$\frac{m_{op}}{m^*} = 1 - \frac{\alpha r_s}{\pi}\int_0^2 \frac{q}{2} F(qa)\,dq + \frac{\alpha r_s}{\pi}\int_0^2 \frac{F(qa)}{q\epsilon_s(q, 0)}\,dq + \frac{\alpha r_s}{2\pi}\int_0^\infty dq \int_0^\infty \frac{d\omega}{2\pi} F(qa)\left(1 - \frac{1}{\epsilon_s(q, i\omega q)}\right) \times \left(\ln\frac{(q+2)^2+\omega^2}{(q-2)^2+\omega^2} - \frac{4(q+2)}{(q+2)^2+\omega^2} - \frac{4(q-2)}{(q-2)^2+\omega^2}\right) \ . \tag{A11}$$

The spin susceptibility $m^* g^*/m_{op} g$ can be obtained by the use of Landau's Fermi-liquid theory. After differentiating the self-energy with respect to $n_{k'\sigma'\nu'}$, one gets part of Landau's f function which is proportional to $\delta_{\sigma\sigma'}\delta_{\nu\nu'}$.

$$f_e(\vec{k}, \vec{k}') = \delta_{\sigma\sigma'}\delta_{\nu\nu'}\left\{-\frac{V(\vec{k}-\vec{k}')}{\epsilon_s(\vec{k}-\vec{k}', \hbar^2k^2/2m_{op} - \hbar^2k'^2/2m_{op})} + \sum_q \int \frac{d\omega}{2\pi i} V(q) G_0^{\sigma\nu}\left(\vec{k}+\vec{q}, \frac{\hbar^2k^2}{2m_{op}} + \omega\right) \frac{\Gamma_{q\nu}(q, \omega)}{\epsilon_s(q, \omega)} \frac{V[(q^2+k_F^2)^{1/2}]}{\epsilon_{TF}[(q^2+k_F^2)^{1/2}]} \times \left[G_0^{\sigma\nu}\left(\vec{k}'+\vec{q}, \frac{\hbar^2k'^2}{2m_{op}} + \omega\right) + G_0^{\sigma\nu}\left(\vec{k}'-\vec{q}, \frac{\hbar^2k'^2}{2m_{op}} - \omega\right)\right]\right\} . \tag{A12}$$

By using the relation

$$\frac{m_{op}g}{m^*g^*} = \frac{m_{op}}{m^*} + \frac{m_{op}k_F}{\hbar^2}\int \frac{d\Omega_{\vec{k}}}{(2\pi)^3} f_e(\vec{k}, \vec{k}')\big|_{k=k'=k_F} \ , \tag{A13}$$

one gets

$$\frac{m_{op}g}{m^*g^*} = \frac{m_{op}}{m^*} - \frac{\alpha r_s}{\pi}\int_0^2 \frac{F(qa)}{q\epsilon_s(q, 0)}\,dq + \frac{\alpha^2 r_s^2}{2\pi^2}\int_0^\infty q\,dq \int_0^\infty \frac{d\omega}{2\pi} F(qa) F[(q^2+1)^{1/2}\beta] \frac{1}{q^2\epsilon_s(q, i\omega q)} \times \frac{\Gamma(q, i\omega q)}{q^2 + 1 + (2/\pi) n_v n_s \alpha r_s F[(q^2+1)^{1/2}a]} \left(\ln\frac{(q+2)^2+\omega^2}{(q-2)^2+\omega^2}\right)^2 \ , \tag{A14}$$

where

$$\Gamma(q, i\omega q)^{-1} = 1 - \frac{2}{\pi}\alpha r_s \frac{F[(q^2+1)^{1/2}a]}{q^2 + 1 + (2/\pi) n_v n_s \alpha r_s F[(q^2+1)^{1/2}a]} \Pi_0(q, i\omega q) \ . \tag{A15}$$

In order to calculate the self-energy shift of electrons in the higher four valleys, one has to put

$$G_0^{\sigma\nu}(\vec{k}, \epsilon) = (\epsilon - \hbar^2k^2/2m_{op} + i0)^{-1} \ . \tag{A16}$$

Further, the vertex correction in the self-energy part vanishes. Therefore one gets

$$\Sigma'_{\sigma\nu}(\vec{k}, \hbar^2k^2/2m_{op}) = \sum_q \int \frac{d\omega}{2\pi i} V(q) \frac{G_0^{\sigma\nu}(\vec{k}+\vec{q}, \hbar^2k^2/2m_{op} + \omega)}{\epsilon(q, \omega)} \ . \tag{A17}$$

At $k=0$ it becomes

$$\Sigma'(0,0) = -\frac{m_{op}}{m\kappa^2}\frac{1}{\pi\alpha r_s}\int_0^\infty dq \int \frac{d\omega}{2\pi} F(qa)\left(1-\frac{1}{\epsilon(q,i\omega q)}\right)\frac{8q}{q^2+\omega^2}\ \mathrm{Ry}\ , \tag{A18}$$

where

$$\epsilon(q,i\omega q) = 1 + (2/\pi)\alpha r_s (n_v n_s/q^2) F(qa)\Gamma(q,i\omega q)\Pi_0(q,i\omega q)\ . \tag{A19}$$

Note added in proof: A recent measurement of the capacitance has revealed that $N_{depl} = 1.0\times10^{11}$ cm^{-2}, which is smaller than the equilibrium value.

---

*Permanent address: Dept. of Physics, University of Tokyo, Bunkyo-ku, Tokyo 113, Japan.

[1]F. Stern and W. E. Howard, Phys. Rev. 163, 816 (1967).
[2]J. A. Pals, Phys. Rev. B 5, 4208 (1972).
[3]G. A. Baraff and J. A. Appelbaum, Phys. Rev. B 5, 476 (1972).
[4]F. Stern, Phys. Rev. B 5, 4891 (1972); Phys. Rev. Lett. 21, 1687 (1968).
[5]F. Stern, Phys. Rev. Lett. 33, 960 (1974).
[6]T. Ando, J. Phys. Soc. Jpn. 39, 411 (1975).
[7]E. Bangert, K. von Klitzing, and G. Landwehr, in *Proceedings of the Twelfth International Conference on Semiconductor Physics, Stuttgart, West Germany*, 1974 (B. G. Teubner, Stuttgart, 1974), p. 714.
[8]F. J. Ohkawa and Y. Uemura, Prog. Theor. Phys. Suppl. 57, 164 (1975).
[9]F. F. Fang and P. J. Stiles, Phys. Rev. 174, 823 (1968).
[10]J. L. Smith and P. J. Stiles, Phys. Rev. Lett. 29 102 (1972).
[11]A. A. Lakhani and P. J. Stiles, Phys. Rev. Lett. 31, 25 (1973).
[12]M. Kobayashi and K. F. Komatsubara, Jpn. J. Appl. Phys. Suppl. 2, 343 (1974).
[13]T. Neugebauer, K. von Klitzing, G. Landwehr, and G. Dorda, Solid State Commun. 17, 295 (1975).
[14]J. F. Janak, Phys. Rev. 178, 1416 (1969).
[15]K. Suzuki and Y. Kawamoto, J. Phys. Soc. Jpn. 35, 1456 (1973).
[16]T. Ando and Y. Uemura, J. Phys. Soc. Jpn. 37, 1044 (1974).
[17]C. S. Ting, T. K. Lee, and J. J. Quinn, Phys. Rev. Lett. 34, 870 (1975).
[18]B. Vinter, Phys. Rev. Lett. 35, 598 (1975).
[19]T. K. Lee, C. S. Ting, and J. J. Quinn, Solid State Commun. 16, 1309 (1975).
[20]A. Kamgar, P. Kneschaurek, G. Dorda, and J. F. Koch, Phys. Rev. Lett. 32, 1251 (1974).
[21]A. Kamgar, P. Kneschaurek, W. Beinvogl, and J. F. Koch, in Ref. 7, p. 709.
[22]J. F. Koch, in *Festkörper-Probleme XV (Advances in Solid State Physics)*, edited by H. J. Queisser (Pergamon/Vieweg, Braunschweig, 1975), p. 79.
[23]P. Kneschaurek, A. Kamgar, and J. F. Koch, Phys. Rev. B (to be published).
[24]F. Stern, Phys. Rev. Lett. 30, 278 (1973).
[25]F. Stern, in Ref. 12, p. 323.
[26]P. Hohenberg and W. Kohn, Phys. Rev. 136, B864 (1964).
[27]W. Kohn and L. J. Sham, Phys. Rev. 140, A1133 (1965).
[28]L. J. Sham and W. Kohn, Phys. Rev. 145, 561 (1966).
[29]See, for example, N. D. Lang, Solid State Phys. 28, 225 (1973).
[30]M. Combescot and P. Nozières, J. Phys. C 5, 2369 (1972).
[31]W. F. Brinkman and T. M. Rice, Phys. Rev. B 7, 1508 (1973).
[32]J. Hubbard, Proc. R. Soc. A 243, 336 (1957).
[33]L. Hedin and B. I. Lundquist, J. Phys. C 4, 2064 (1971).
[34]R. G. Wheeler and H. S. Goldberg, IEEE Trans. Electron Devices (to be published).
[35]S. Ma and K. A. Brueckner, Phys. Rev. 165, 18 (1968); F. Herman, J. P. Van Dyke, and I. B. Ortenburger, Phys. Rev. Lett. 22, 807 (1969); L. J. Sham, Phys. Rev. B 7, 4357 (1973); L. Kleinman, *ibid.* B 10, 2221 (1974); M. Rasolt and S. H. Vosko, *ibid.* B 10, 4195 (1974).
[36]T. M. Rice, Ann. Phys. (N. Y.) 31, 100 (1965).